NANO LETTERS

Letter

pubs.acs.org/NanoLett

Understanding the Role of Different Conductive Polymers in Improving the Nanostructured Sulfur Cathode Performance

Weiyang Li,[†] Qianfan Zhang,[‡] Guangyuan Zheng,[§] Zhi Wei Seh,[†] Hongbin Yao,[†] and Yi Cui*[,†,∥]

[†]Department of Materials Science and Engineering, Stanford University, Stanford, California 94305, United States

[‡]School of Materials Science and Engineering, Beihang University, Beijing, 100191, P. R. China

[§]Department of Chemical Engineering, Stanford University, Stanford, California 94305, United States

[∥]Stanford Institute for Materials and Energy Sciences, SLAC National Accelerator Laboratory, 2575 Sand Hill Road, Menlo Park, California 94025, United States

Supporting Information

ABSTRACT: Lithium sulfur batteries have brought significant advancement to the current state-of-art battery technologies because of their high theoretical specific energy, but their wide-scale implementation has been impeded by a series of challenges, especially the dissolution of intermediate polysulfides species into the electrolyte. Conductive polymers in combination with nanostructured sulfur have attracted great interest as promising matrices for the confinement of lithium polysulfides. However, the roles of different conductive polymers on the electrochemical performances of sulfur electrode remain elusive and poorly understood due to the vastly different structural configurations of conductive polymer−sulfur composites employed in previous studies. In this work, we systematically investigate the influence of different conductive polymers on the sulfur cathode based on conductive polymer-coated hollow sulfur nanospheres with high uniformity. Three of the most well-known conductive polymers, polyaniline (PANI), polypyrrole (PPY), and poly(3,4-ethylenedioxythiophene) (PEDOT), were coated, respectively, onto monodisperse hollow sulfur nanopsheres through a facile, versatile, and scalable polymerization process. The sulfur cathodes made from these well-defined sulfur nanoparticles act as ideal platforms to study and compare how coating thickness, chemical bonding, and the conductivity of the polymers affected the sulfur cathode performances from both experimental observations and theoretical simulations. We found that the capability of these three polymers in improving long-term cycling stability and high-rate performance of the sulfur cathode decreased in the order of PEDOT > PPY > PANI. High specific capacities and excellent cycle life were demonstrated for sulfur cathodes made from these conductive polymer-coated hollow sulfur nanospheres.

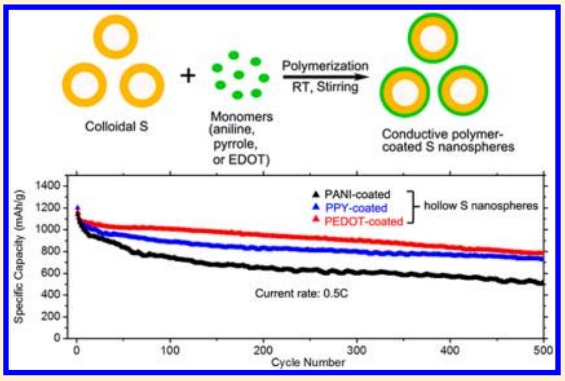

KEYWORDS: *Lithium sulfur battery, energy storage, conductive polymer, nanostructure*

Rechargeable lithium-ion batteries currently dominate the portable consumer electronics market owing to their high energy density, long lifespan, and flexible and lightweight design. However, presently available lithium-ion batteries based on lithium metal oxides (or phosphates) and carbon systems with theoretical specific energy of about 400 W·h/kg cannot satisfy the increasing energy demand of modern society, especially battery requirements for extended-range electric vehicles.[1−3] High energy storage is also important in reducing the cost per stored energy for grid energy storage.[4] Among the best candidates for next generation high energy storage systems, the lithium sulfur battery is especially attractive because of its high theoretical specific energy (around 2600 W·h/kg) and cost savings.[5] Sulfur cathode has a theoretical capacity of 1673 mA·h/g, more than 5 times higher than that of $LiCoO_2$. In addition, sulfur is abundant in nature, low cost, and low toxicity. Despite all of these advantages, the practical application of lithium sulfur batteries to date has been hindered by a series of obstacles, including poor cycle life, low Coulombic efficiency, and low active material utilization.[5−10] These problems are mainly caused by multiple materials challenges, including large volumetric expansion of sulfur upon lithiation, dissolution of lithium polysulfides in the electrolyte, and low ionic/electronic conductivity of both sulfur and lithium sulfide.

To overcome these problems, extensive research has been conducted with focus on controlling the electrode structure and composition. Ever since the successful demonstration of improving sulfur cathode performance using ordered mesoporous carbon,[11] various carbon micro/nanostructured materials, such as mesoporous carbon spheres,[12−14] hollow/porous carbon nanofibers,[15−18] activated carbon fiber,[19] microporous

Received: August 21, 2013
Revised: September 16, 2013
Published: October 15, 2013

carbon paper,[20] and graphene oxides,[21,22] have been studied as a conductive matrix to constrain sulfur within the carbon frameworks. On one hand, these carbon-based materials effectively enhanced the conductivity of the electrode and could trap polysulfides to some extent. On the other hand, further research showed that carbon could not serve as an ideal matrix. Our recent study showed that lithiation of sulfur could cause detachment of lithium sulfide from the carbon surface during discharge due to the low binding energy between the nonpolar carbon and polar Li_xS ($0 < x \leq 2$) clusters, resulting in loss of electrical contact and capacity decay.[23] Therefore, additional polymer modification on carbon surface or a layer of polymer coating on the carbon/sulfur composites was essential to stabilize the cycling performance of the sulfur cathode.[11,23] Moreover, various metal oxides have also been studied as alternatives to carbon[24−26] with a particular example of sulfur−TiO_2 yolk-shell nanostructures showing outstanding performance.[27]

Conductive polymers, indeed, have been explored as promising alternative matrices to carbon for sulfur entrapment.[28−33] Of notable examples include the work by Liu et al., who reported the use of polyaniline nanotubes for sulfur encapsulation, which showed impressive cycle life at high rate (a capacity of 432 mAh/g at 1C after 500 cycles);[28] Manthiram and Fu reported a core−shell structured sulfur−polypyrrole composite cathode, which gives a capacity of over 400 mAh/g at 2C after 50 cycles;[29] Chen et al. recently showed that small sulfur nanoparticles (10−20 nm) wrapped with poly(3,4-ethylenedioxythiophene) exhibited a capacity retention of 80% at C/4 after 50 cycles.[30] Although a variety of conductive polymers were studied, no attempt has been made to systematically compare and understand the roles of different conductive polymers on the electrochemical performances of the sulfur cathode due to the varied structural configurations of conductive polymer−sulfur composites employed in previous reports. Therefore, it would be a great advantage to have a well-defined structure as an ideal platform to study effects of conductive polymers on sulfur electrode from both fundamental and practical perspectives.

Most recently, our group demonstrated the fabrication of monodisperse polyvinylpyrrolidone (PVP)-encapsulated hollow sulfur nanospheres for the sulfur cathode, which could improve the cycling stability due to the void space engineered into the PVP shell to accommodate the sulfur volume expansion.[34] However, the rate capability is relatively weak due to the nonconductive PVP shells on the surfaces of sulfur particles. Herein we present stable and high performance sulfur cathodes made from conductive polymer-coated hollow sulfur nanospheres. Polyaniline (PANI), polypyrrole (PPY), and poly(3,4-ethylenedioxythiophene) (PEDOT), three of the most well-known conductive polymers, were coated, respectively, onto monodisperse hollow sulfur nanopsheres through a facile, versatile, and scalable polymerization process in aqueous solution at room temperature. Since all of the conductive polymer-encapsulated sulfur particles in our system possess the same hollow structure except with different coatings, they act as ideal models to accurately compare the influence of different conductive polymers on the sulfur cathode by ruling out the factor of sulfur volume expansion. We systematically investigated how coating thickness and conductivity of these polymers affected the electrochemical properties of sulfur electrodes. We also performed ab initio simulations to elucidate the significance of chemical bonding between these conductive polymers and Li_xS ($0 < x \leq 2$) species in enhancing the cycling stability. Comparing the performances of the cells made from PANI-, PPY-, and PEDOT-encapsulated hollow sulfur nanospheres, we found that the ability of these three polymers in enabling long cycle life and high-rate performance decreased in the order of PEDOT > PPY > PANI. After 500 discharge/charge cycles at C/2 rate, the cells made from PEDOT- and PPY-encapsulated hollow sulfur nanospheres still delivered high reversible capacities of 780 and 726 mAh/g, respectively (a decay of only 0.066% and 0.08% per cycle). As to rate capability, even at high current of 4C, a capacity of 624, 440, and 329 mAh/g can be achieved for the cells made from PEDOT-, PPY-, and PANI-coated sulfur particles, respectively.

Figure 1a schematically illustrates the procedure we used for fabricating the conductive polymer-coated hollow sulfur nanospheres. In a typical synthesis, monodisperse hollow sulfur nanospheres developed in our previous report were dispersed in water,[34] to which monomers (aniline, pyrrole, or 3,4-ethylenedioxythiophene (EDOT)), a small amount of acid

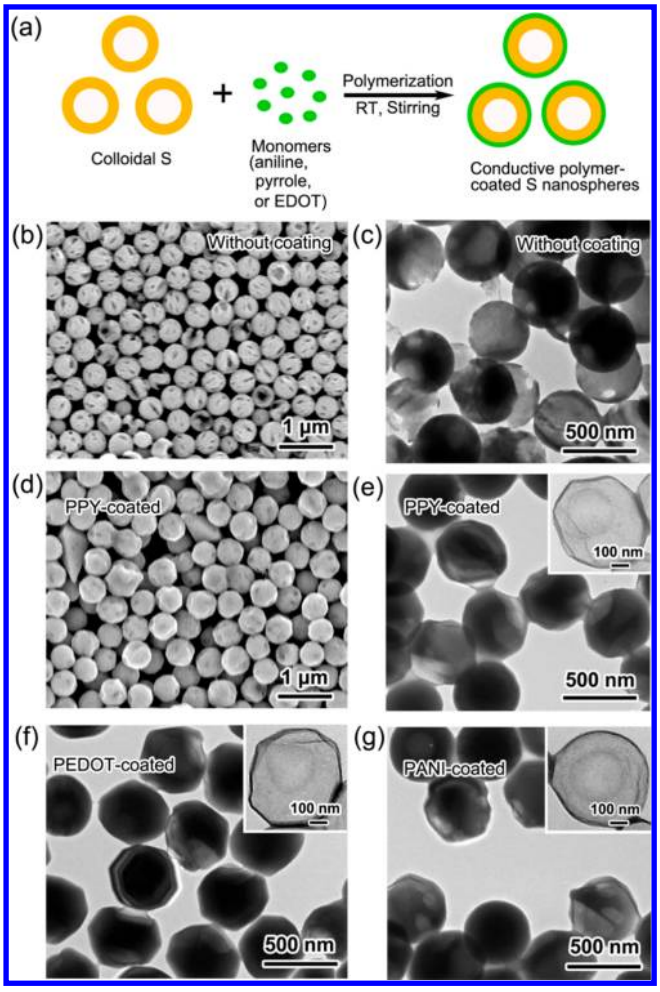

Figure 1. (a) Schematic illustration of the fabrication process of conductive polymer-coated hollow sulfur nanospheres. RT, room temperature. (b, d) Scanning electron microscopy (SEM) and (c, e) transmission electron microscopy (TEM) images of the hollow sulfur nanospheres (b, c) before and (d, e) after coating with polypyrrole (PPY). (f, g) TEM images of the (f) poly(3,4-ethylenedioxythiophene) (PEDOT)- and (g) polyaniline (PANI)-coated hollow sulfur nanospheres. Insets in e−g: TEM images of the PPY, PEDOT, and PANI shell after dissolving sulfur with toluene.

dx.doi.org/10.1021/nl403130h | *Nano Lett.* 2013, 13, 5534−5540

(hydrochloric acid for aniline; camphorsulfonic acid for EDOT; no acid needed for pyrrole), and oxidant ($FeCl_3$ for pyrrole; $(NH_4)_2S_2O_8$ for aniline and EDOT) were added. The mixture solution was stirred at room temperature overnight, and then PANI-, PPY-, or PEDOT-coated hollow sulfur nanospheres were formed depending on which corresponding monomer was used for the synthesis.

Figure 1b–e show typical scanning electron microscopy (SEM) and transmission electron microscopy (TEM) images of the hollow sulfur nanospheres before and after PPY coating. Before coating with conductive polymers (Figure 1b and c), the sulfur particles exhibited a well-defined spherical shape with hollow interiors. Besides the large empty space in the middle, these sulfur particles also have small pores in their walls as described in our previous report.[34] After coating with a layer of PPY (Figure 1d and e), the monodispersity, the spherical morphology , and the hollow characteristic (determined from the distinct contrast in the TEM image) of the sulfur particles are all well-preserved. The small pores in the walls became less obvious as shown in the SEM image (Figure 1d), indicating the PPY coating on the particle surface. To clearly reveal the PPY shell, we used toluene to dissolve sulfur away, showing that the thickness of the PPY shell is ~20 nm (inset in Figure 1e). Moreover, the morphologies of both PEDOT- and PANI-coated hollow sulfur nanospheres are similar to that of the PPY-coated ones, as shown in the TEM images in Figure 1f and g. The coating thicknesses of PEDOT and PANI on the sulfur nanospheres are the same as the PPY coating, which are also ~20 nm (insets in Figure 1f and g, revealing the PEDOT and PANI shell after dissolving sulfur by toluene). The respective amount of elemental sulfur in PANI-, PPY-, and PEDOT-coated sulfur nanospheres is ~74, 77, and 78 wt % through thermogravimetric analysis.

To evaluate the electrochemical performance of the conductive polymer-coated sulfur nanoparticles, 2032-type coin cells were assembled using a metallic lithium foil as the counter electrode. The electrolyte used was lithium bis-(trifluoromethanesulfonyl)imide in 1:1 (v/v) 1,2-dimethoxy-ethane and 1,3-dioxolane. $LiNO_3$ (1 wt %) was added to the electrolyte as an additive to help passivate the surface of the lithium anode and reduce the shuttle effect.[9,35] The typical mass loading of sulfur was ~1.5 mg cm^{-2}, and specific capacities were calculated based on the sulfur mass only.

Figure 2a shows the cycling performances (discharge capacity vs cycle number) of the cells made from PANI-, PPY-, and PEDOT-encapsulated hollow sulfur nanospheres at C/5 current rate for 300 cycles. For simplicity, the electrodes made from these three samples are referred as PANI-S, PPY-S, and PEDOT-S in the following content. At C/5, the cells made from PANI-S, PPY-S, and PEDOT-S all exhibited high initial discharge capacities of 1355, 1315, and 1285 mAh/g, respectively. After 100 cycles of charge/discharge, a reversible capacity of 876, 923, and 1071 mAh/g was retained for PANI-S, PPY-S, and PEDOT-S, respectively. Relative to the initial cycle, the capacity retention achieved at the end of 100 cycles for these cells decreased in the following order: PEDOT-S (83%) > PPY-S (70%) > PANI-S (65%). Even after 300 cycles, a high reversible capacity of around 860, 808, and 711 mAh/g was still attained for PEDOT-S, PPY-S, and PANI-S, respectively, corresponding to a capacity retention of 67%, 61%, and 52% of their respective initial capacities. The average Coulombic efficiencies of the three cells at C/5 for 300 cycles are 99.6% (PEDOT-S), 99.2% (PPY-S), and 98.5% (PANI-S) (Figure S1). It is noted that PANI, PPY, and PEDOT were reported to be electrochemically active with lithium ions in the range of 2.5–4 V (the oxidized potentials vs Li/Li^+ are above 3 V),[36–40] which is beyond the electrochemical window of lithium sulfur battery.

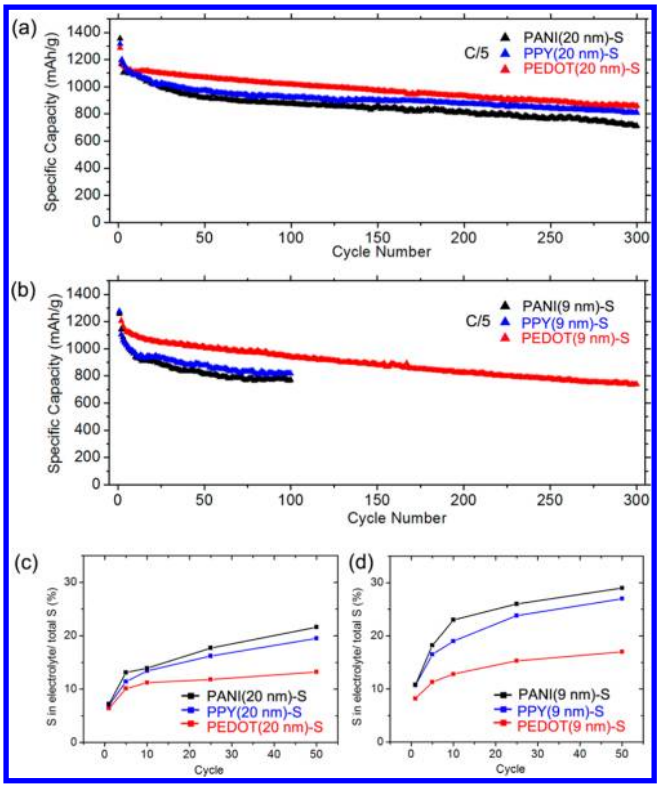

Figure 2. (a, b) Cycling performances of the cells made from hollow sulfur nanospheres with PANI, PPY, and PEDOT coatings of (a) ~20 nm and (b) ~9 nm at C/5 rate over 300 cycles. (c, d) Percentage of sulfur in the electrolyte relative to the total sulfur mass on the electrode for the cells made from the sulfur nanospheres with (c) 20 nm and (d) 9 nm conductive polymer coatings at the end of 1st, 5th, 10th, 25th, and 50th cycle (at fully discharged state) at C/5. 1C = 1673 mA/g.

To further understand the effect of polymer encapsulation, we decreased the thickness of the conductive polymer coatings on the sulfur particle surface by shortening the reaction time of polymerization. Figure 2b shows the cycling performances of the cells made from hollow sulfur nanospheres with conductive polymer coatings of ~9 nm at a C/5 rate. It can be observed that the sulfur nanospheres with thinner coatings all showed faster capacity decay than the ones with thicker coatings (Figure 2a). It is noted that PEDOT is the best among the three conductive polymers to stabilize the sulfur cathode cycling performance at both coating thicknesses, while PANI and PPY showed similar performances, especially during the first 100 cycles. Even when the coating is only 9 nm, the cell made from PEDOT-S still showed an initial capacity of 1267 mAh/g, and a high capacity of 940 mAh/g was attained after 100 cycles (a capacity retention of 74%). Even after 300 cycles, a reversible capacity of 739 mAh/g can still be achieved. In comparison, PPY-S and PANI-S with 9 nm coatings decays to 822 and 765 mAh/g (capacity retention of 64% and 60%, respectively) within 100 cycles. This clearly demonstrated that a higher level of conductive polymer encapsulation obviously contributes to a lower degree of polysulfide dissolution and thus reduces the loss of active materials. This is also supported

dx.doi.org/10.1021/nl403130h | Nano Lett. 2013, 13, 5534–5540

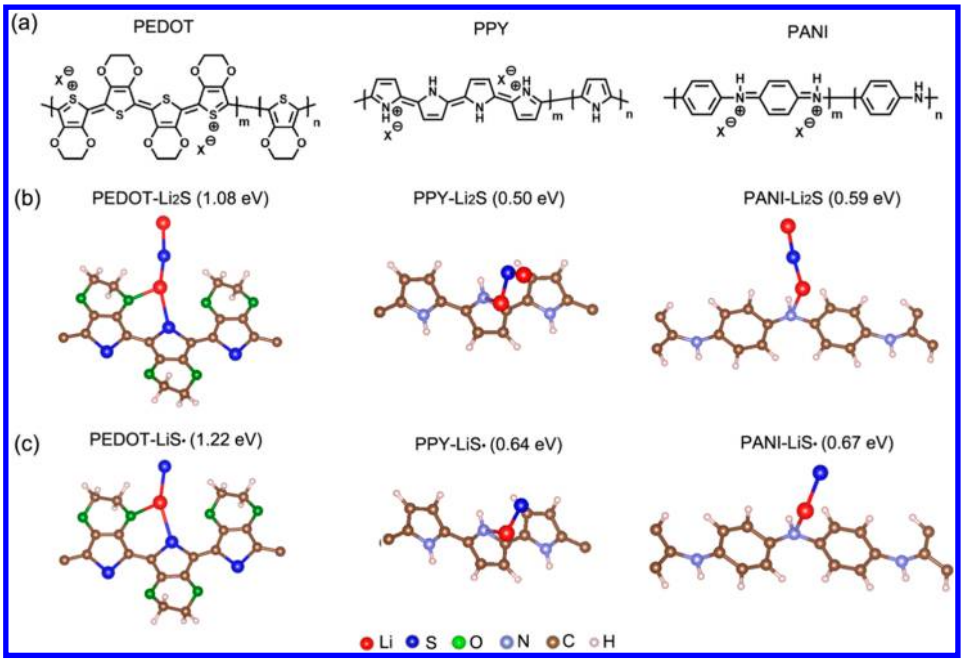

Figure 3. (a) Chemical structures of PEDOT, PPY, and PANI. m and n indicate the doped and undoped parts in these polymers, and X indicates the counterion incorporated during polymerization. (b, c) Ab initio simulations showing the most stable configurations and calculated binding energies of (b) Li_2S and (c) Li–S· species with the heteroatoms (oxygen, sulfur, or nitrogen) in PEDOT, PPY, and PANI. The corresponding binding energies are displayed in parentheses.

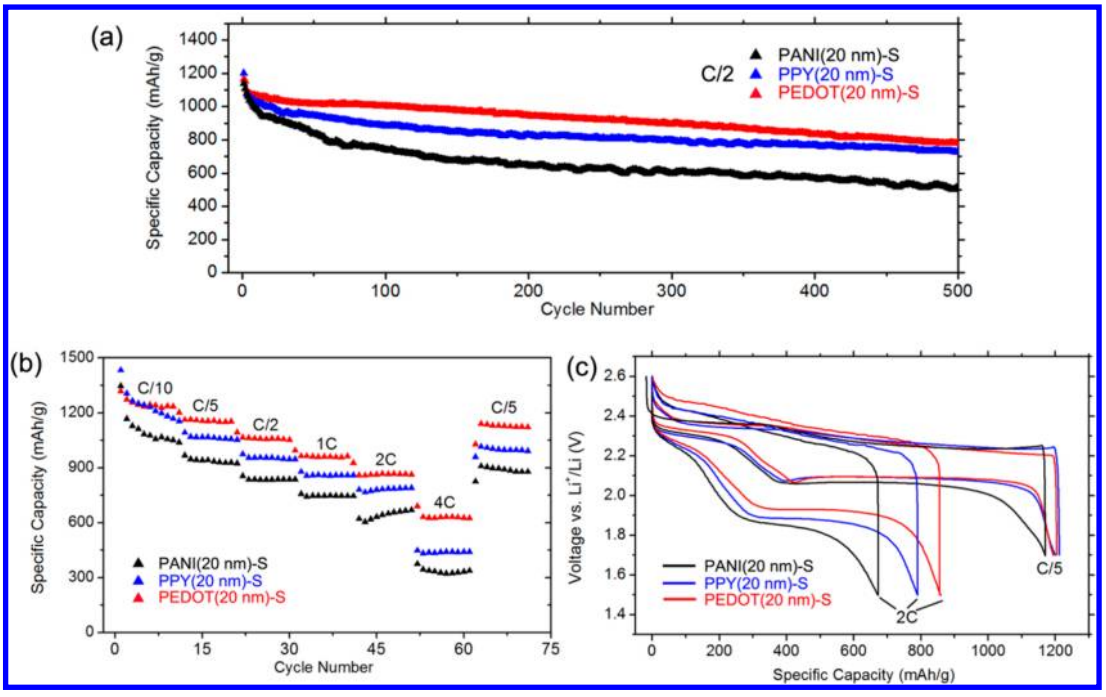

Figure 4. (a) Cycling performances of the cells made from hollow sulfur nanospheres with PANI, PPY, and PEDOT coatings of ~20 nm at C/2 rate for 500 cycles. (b) Rate capability of the cells discharged at various current rates from C/10 to 4C. (c) Typical discharge–charge voltage profiles of the cells at C/5 and 2C (1C = 1673 mA/g).

by measuring the sulfur content in the electrolyte by the end of discharge using inductively coupled plasma-optical emission spectroscopy (ICP-OES), which provides information about the degree of polysulfide dissolution. In a typical experiment, the coin cells were dissembled in argon-filled glovebox, and then the components of the cells (cathode, anode, and separator) were washed with 1,3-dioxolane. This polysulfide-containing solution was oxidized with concentrated nitric acid and then diluted with deionized water for analysis of sulfur content using ICP-OES. ICP-OES analysis (Figure 2c and d) showed a consistently higher percentage loss of sulfur into the electrolyte at various stages of cycling (at the end of 1, 5, 10, 25, and 50 cycles, at fully discharged state) for cells made from the sulfur nanospheres with 9 nm conductive polymer coatings compared to those with 20 nm coatings. It is also worth mentioning that, even with a thin layer of PEDOT coating (9

dx.doi.org/10.1021/nl403130h | *Nano Lett.* 2013, 13, 5534–5540

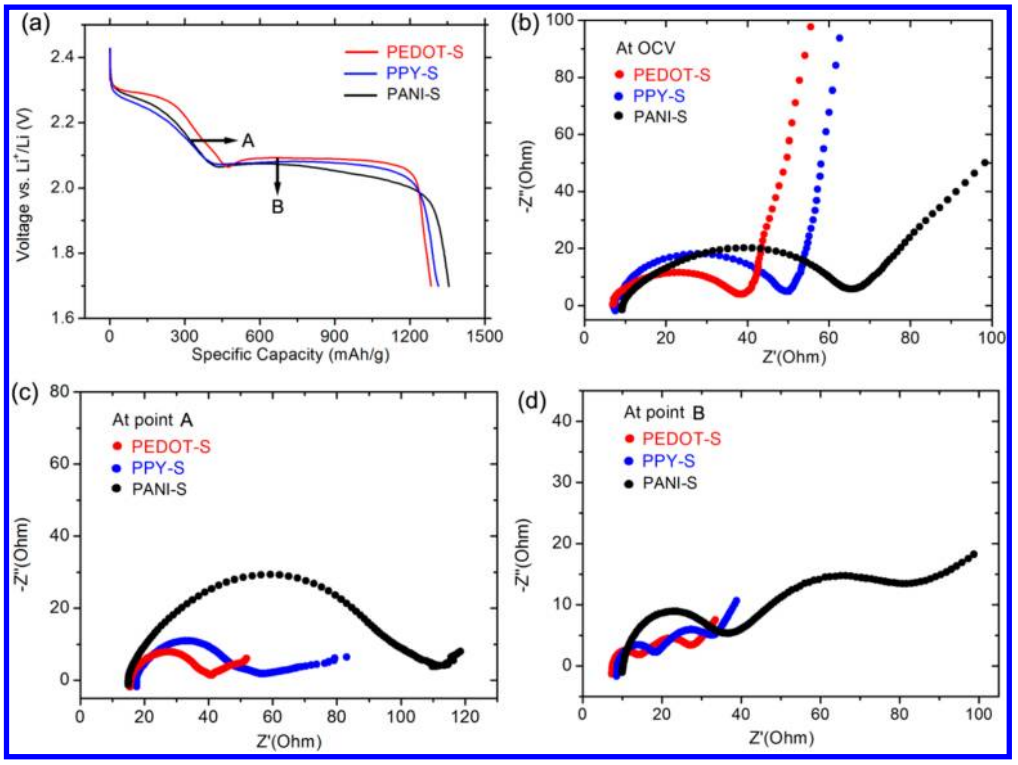

Figure 5. (a) Discharge voltage profiles of the sulfur cathode made from PANI-, PPY-, and PEDOT-encapsulated hollow sulfur nanospheres during the first discharge at C/5. (b–d) Nyquist plots for the sulfur cathode made from PANI-, PPY-, and PEDOT-encapsulated hollow sulfur nanospheres in the frequency range of 100 mHz to 200 kHz during the first discharge at different states: (b) open circuit voltage (OCV), (c) point A and (d) point B marked in a.

nm), only 17% of the sulfur was found to dissolve in the electrolyte after 50 cycles, which is much lower than those with 9-nm coatings of PPY and PANI (about 27% and 29%), as shown in Figure 2d. This indicates that, besides the physical confinement of polysulfide dissolution, the chemical interaction between PEDOT and polysulfides must play an essential role in stabilizing the cycling performance.

To elucidate the interaction between Li_xS ($0 < x \leq 2$) species and conductive polymers (PEDOT, PPY, and PANI), we then performed ab initio simulations in the framework of density functional theory.[41−45] Our previous study showed the interaction between Li_2S and the functional groups in macromolecular binders greatly affected the cycling stability of Li_2S cathode.[46] Figure 3a shows the chemical structures of PEDOT, PPY, and PANI, in which m and n indicate the doped and undoped parts in these polymers (X indicates the counterion incorporated during polymerization). In general, the heteroatoms with lone electron pairs (such as oxygen, nitrogen, and sulfur atoms) are able to bind with the lithium atom in Li_xS ($0 < x \leq 2$), whereas carbon, hydrogen, and the heteroatoms at the oxidized (doped) state (S^+ for PEDOT and N^+ for PANI/PPY) show weak interaction with Li_xS clusters. For simplicity, we chose the repeating unit of unoxidized (undoped) form of each polymer as the modeling molecule to compute the binding energy so as to represent the interaction between these polymers and Li_xS ($0 < x \leq 2$) species. This simulation might not give us an absolute quantification of the binding strength but will provide a qualitative understanding on the influence of chemical bonding on the cycling stability of the sulfur cathode. The results are summarized in Figure 3b and c. As to PEDOT, we can see that both oxygen and sulfur atom strongly bind with the lithium atom in Li_2S to form a chelated coordination structure. This very stable configuration gives a strong binding energy of 1.22 eV. In comparison, both PANI and PPY were found to have weaker interaction with Li_2S, because there is only separate $\pi-\sigma$ coordination between heteroatoms and the lithium atom. The respective binding energies are much lower, 0.67 eV for PANI and 0.64 eV for PPY. Moreover, a similar phenomenon can be observed in the interaction between conductive polymers and Li−S· species, which represent the relevant end groups in the general class of lithium polysulfides (Li−S−S_{n-2}−S−Li; Li_2S_n in short, $4 \leq n \leq 8$). Because of the stability difference between chelation and separate coordination, PEDOT shows a much stronger binding energy (1.08 eV) with the lithium atom in Li−S· than PANI (0.59 eV) and PPY (0.50 eV). This strong binding affinity of PEDOT with Li_xS ($0 < x \leq 2$) can effectively reduce the polysulfide diffusion into the electrolyte and thus contribute to a more stable cycling performance compared to PPY and PANI, which is consistent with the results shown in Figure 2.

To further evaluate the electrode kinetics and stability, we cycled the cells at various current rates. Figure 4a shows the cycling performances (discharge capacity vs cycle number) of the cells made from PANI-S, PPY-S, and PEDOT-S with conductive polymer coatings of ~20 nm at a higher current rate C/2 for 500 cycles. The cells made from PANI-S, PPY-S, and PEDOT-S still delivered high initial discharge capacities of 1140, 1201, and 1165 mAh/g, respectively. After 100 cycles of charge/discharge, a reversible capacity of about 740, 885, and 1004 mAh/g can be obtained for PANI-S, PPY-S, and PEDOT-S (capacity retention of 65%, 74%, and 86%), respectively, indicating a slightly slower capacity decay than the ones cycled at C/5 (Figure 2a). Even after 500 cycles of charge/discharge, the cells made from PEDOT-S and PPY-S still delivered high

dx.doi.org/10.1021/nl403130h | Nano Lett. 2013, 13, 5534−5540

reversible discharge capacities of 780 and 726 mAh/g, respectively, corresponding to capacity retention of 67% and 60% (a decay of only 0.066% and 0.08% per cycle). In contrast, the cell made from PANI-S showed a relatively faster capacity decay, which gave a capacity of 516 mAh/g (corresponding to a capacity retention of 45%, a decay of 0.11% per cycle). Compared to the cycle life shown in Figure 2a, the difference in the cycling stability between PEDOT-S, PPY-S, and PANI-S became more obvious when cycled at higher current rates. The rate capability performances of the cells are shown in Figure 4b. When first discharged the cells at C/10 for 10 cycles, the cells made from PANI-S, PPY-S, and PEDOT-S showed a reversible capacity of 1051, 1168, and 1234 mAh/g, respectively. Subsequent cycling at C/5, C/2, 1C, 2C, and 4C (each rate for 10 cycles) clearly reveals that the rate capability of the cells are ordered as follows: PEDOT-S > PPY-S > PANI-S. This is also supported by the typical voltage profiles of these cells at C/5 and 2C rates (Figure 4c). At both rates, the voltage hysteresis between the charge and the discharge curves decreases in the order of PANI-S > PPY-S > PEDOT-S. At a high current rate of 2C, the PEDOT-S and PPY-S can give a reversible capacity of 858 and 789 mAh/g, which is much higher than that of the PANI-S, about 666 mAh/g. When the current was further increased to 4C, a high capacity of 624 mAh/g can still be achieved for PEDOT-S, indicating fast reaction kinetics; while PPY-S and PANI-S only showed capacities of 440 and 329 mAh/g. It is worth mentioning that when the current was abruptly switched from 4C to C/5 again, more than 96% of the original capacities were recovered for all three cells (Figure 4b), indicating the superior robustness and reversibility of these electrodes.

It is known that the electrode kinetics is mainly determined by the conductivity of the whole electrode. In our system, the structures of the PANI-S, PPY-S, and PEDOT-S electrodes are the same except the polymer coatings on the hollow sulfur nanospheres (the coating thicknesses were also maintained the same). Therefore, the rate capability of the electrode is mainly determined by the conductivity of the polymers. We further carried out electrochemical impedance spectroscopy (EIS) measurements of the PANI-, PPY-, and PEDOT-encapsulated hollow sulfur nanosphere electrodes at different discharge states (at open circuit voltage, at the upper and lower voltage plateaus) during the first discharge, as shown in Figure 5. For all three electrodes, two depressed semicircles were observed during the discharge process. Previous studies showed that the semicircle in the high-frequency (HF) region could reflect the charge transfer process at the conductive agent interface which dominates the reduction reaction during upper voltage plateau, while the semicircle in the middle frequency (MF) range could be attributed to the mass transport which dominates the lower voltage plateau (formation of insoluble polysulfide species).[9,47] As shown in Figure 5b–d, the charge transfer resistances of the three electrodes at different discharged states all increase in the order of PEDOT-S < PPY-S < PANI-S. Especially for PANI-S, it has a much higher charge transfer resistance than that of PEDOT-S and PPY-S. The EIS results are in good agreement with what we observed for the rate capability of these cells. This also reveals that the conductivity of the three polymers in our system decreased in the order of PEDOT > PPY > PANI.

In summary, we have successfully demonstrated high-performance sulfur cathodes made from PANI-, PPY-, and PEDOT-coated hollow sulfur nanospheres, which act as ideal models to systematically study the effects of different conductive polymers on the electrochemical properties of sulfur electrode. Ab initio simulations were carried out to elucidate the chemical interaction between these conductive polymers and Li_xS ($0 < x \leq 2$) species. Comparing the electrochemical performances of the cells made from these sulfur particles, we found that not only the physical confinement of lithium polysulfides within the conductive polymer shells but also the chemical bonding between the heteroatoms in these polymers with Li_xS ($0 < x \leq 2$) played essential roles in improving the cycling stability. In addition, the conductivity of the polymers greatly determined the rate performance of the sulfur cathode. Among the three conductive polymers, PEDOT was found to be the best choice that can enable a long cycle life and high-rate capability for the sulfur cathode.

■ ASSOCIATED CONTENT

Supporting Information

Detailed description of the experimental procedures and Coulombic efficiencies of the cells made from PANI-, PPY-, and PEDOT-encapsulated hollow sulfur nanospheres at C/5 for 300 cycles. This material is available free of charge via the Internet at http://pubs.acs.org.

■ AUTHOR INFORMATION

Corresponding Author

*E-mail: yicui@stanford.edu.

Notes

The authors declare no competing financial interest.

■ ACKNOWLEDGMENTS

Y.C. acknowledges the support from the Assistant Secretary for Energy Efficiency and Renewable Energy, Office of Vehicle Technologies of the U.S. Department of Energy.

■ REFERENCES

(1) Armand, M.; Tarascon, J. M. *Nature* **2008**, *451*, 652.
(2) Whittingham, M. S. *Chem. Rev.* **2004**, *104*, 4271.
(3) Goodenough, J. B.; Kim, Y. *Chem. Mater.* **2010**, *22*, 587.
(4) Dunn, B.; Kamath, H.; Tarascon, J. M. *Science* **2011**, *334*, 928.
(5) Bruce, P. G.; Freunberger, S. A.; Hardwick, L. J.; Tarascon, J. M. *Nat. Mater.* **2012**, *11*, 19.
(6) Yang, Y.; Zheng, G.; Cui, Y. *Chem. Soc. Rev.* **2013**, *42*, 3018.
(7) Mikhaylik, Y. V.; Akridge, J. R. *J. Electrochem. Soc.* **2004**, *151*, A1969.
(8) Ji, X. L.; Nazar, L. F. *J. Mater. Chem.* **2010**, *20*, 9821.
(9) Barchasz, C.; Lepretre, J. C.; Alloin, F.; Patoux, S. *J. Power Sources* **2012**, *199*, 322.
(10) Shim, J.; Striebel, K. A.; Cairns, E. J. *J. Electrochem. Soc.* **2002**, *149*, A1321.
(11) Ji, X.; Lee, K. T.; Nazar, L. F. *Nat. Mater.* **2009**, *8*, 500.
(12) Jayaprakash, N.; Shen, J.; Moganty, S. S.; Corona, A.; Archer, L. A. *Angew. Chem., Int. Ed.* **2011**, *50*, 5904.
(13) Kim, J.; Lee, D.-J.; Jung, H.-G.; Sun, Y.-K.; Hassoun, J.; Scrosati, B. *Adv. Funct. Mater.* **2013**, *23*, 1076.
(14) Schuster, J.; He, G.; Mandlmeier, B.; Yim, T.; Lee, K. T.; Bein, T.; Nazar, L. F. *Angew. Chem., Int. Ed.* **2012**, *51*, 3591.
(15) Zheng, G.; Yang, Y.; Cha, J. J.; Hong, S. S.; Cui, Y. *Nano Lett.* **2011**, *11*, 4462.
(16) Guo, J.; Xu, Y.; Wang, C. *Nano Lett.* **2011**, *11*, 4288.
(17) Ji, L.; Rao, M.; Aloni, S.; Wang, L.; Cairns, E. J.; Zhang, Y. *Energy Environ. Sci.* **2011**, *4*, 5053.
(18) Zu, C.; Fu, Y.; Manthiram, A. *J. Mater. Chem. A* **2013**, *1*, 10362–10367.

(19) Elazari, R.; Salitra, G.; Garsuch, A.; Panchenko, A.; Aurbach, D. *Adv. Mater.* **2011**, *23*, 5641.
(20) Su, Y.-S.; Manthiram, A. *Nat. Commun.* **2012**, *3*, 1166.
(21) Ji, L.; Rao, M.; Zheng, H.; Zhang, L.; Li, Y.; Duan, W.; Guo, J.; Cairns, E. J.; Zhang, Y. *J. Am. Chem. Soc.* **2011**, *133*, 18522.
(22) Wang, H.; Yang, Y.; Liang, Y.; Robinson, J. T.; Li, Y.; Jackson, A.; Cui, Y.; Dai, H. *Nano Lett.* **2011**, *11*, 2644.
(23) Zheng, G.; Zhang, Q.; Cha, J. J.; Yang, Y.; Li, W.; Seh, Z. W.; Cui, Y. *Nano Lett.* **2013**, *13*, 1265.
(24) Ji, X.; Evers, S.; Black, R.; Nazar, L. F. *Nat. Commun.* **2011**, *2*, 325.
(25) Evers, S.; Yim, T.; Nazar, L. F. *J. Phys. Chem. C* **2012**, *116*, 19653.
(26) Demir-Cakan, R.; Morcrette, M.; Nouar, F.; Davoisne, C.; Devic, T.; Gonbeau, D.; Dominko, R.; Serre, C.; Feryey, G.; Tarascon, J.-M. *J. Am. Chem. Soc.* **2011**, *133*, 16154.
(27) Seh, Z. W.; Li, W.; Cha, J. J.; Zheng, G.; Yang, Y.; McDowell, M. T.; Hsu, P.-C.; Cui, Y. *Nat. Commun.* **2013**, *4*, 1331.
(28) Xiao, L.; Cao, Y.; Xiao, J.; Schwenzer, B.; Engelhard, M. H.; Saraf, L. V.; Nie, Z.; Exarhos, G. J.; Liu, J. *Adv. Mater.* **2012**, *24*, 1176.
(29) Fu, Y.; Manthiram, A. *RSC Adv.* **2012**, *2*, 5927.
(30) Chen, H.; Dong, W.; Ge, J.; Wang, C.; Wu, X.; Lu, W.; Chen, L. *Sci. Rep.* **2013**, *3*, 1910.
(31) Yin, L.; Wang, J.; Lin, F.; Yang, J.; Nuli, Y. *Energy Environ. Sci.* **2012**, *5*, 6966.
(32) Yin, L.; Wang, J.; Yu, X.; Monroe, C. W.; Nuli, Y.; Yang, J. *Chem. Commun.* **2012**, *48*, 7868.
(33) Hwang, T. H.; Jung, D. S.; Kim, J. S.; Kim, B. G.; Choi, J. W. *Nano Lett.* **2013**, *13*, 4532.
(34) Li, W.; Zheng, G.; Yang, Y.; Seh, Z. W.; Liu, N.; Cui, Y. *Proc. Natl. Acad. Sci. U.S.A.* **2013**, *110*, 7148.
(35) Aurbach, D.; Pollak, E.; Elazari, R.; Salitra, G.; Kelley, C. S.; Affinitob, J. *J. Electrochem. Soc.* **2009**, *156*, A694.
(36) Novák, P.; Mueller, K.; Santhanam, K. S. V.; Haas, O. *Chem. Rev.* **1997**, *97*, 207.
(37) Yang, H.; Song, T.; Liu, L.; Devadoss, A.; Xia, F.; Han, H.; Park, H.; Sigmund, W.; Kwon, K.; Paik, U. J. *Phys. Chem. C* **2013**, *117*, 17376.
(38) Chang, C. C.; Her, L. J.; Hong, J. L. *Electrochim. Acta* **2005**, *50*, 4461.
(39) Qie, L.; Yuan, L. X.; Zhang, W. X.; Chen, W. M.; Huang, Y. H. *J. Electrochem. Soc.* **2012**, *159*, A1624.
(40) Jung, H. R.; Lee, W. J. *Solid State Ionics* **2011**, *187*, 50.
(41) Kresse, G.; Hafner, J. *Phys. Rev. B* **1993**, *48*, 13115.
(42) Kresse, G.; Furthmuller, J. *Phys. Rev. B* **1996**, *54*, 11169.
(43) Blochl, P. E. *Phys. Rev. B* **1994**, *50*, 17953.
(44) Perdew, J. P.; Burke, K.; Ernzerhof, M. *Phys. Rev. Lett.* **1996**, *77*, 3865.
(45) Momma, K.; Izumi, F. *J. Appl. Crystallogr.* **2011**, *44*, 1272.
(46) Seh, Z. W.; Zhang, Q.; Li, W.; Zheng, G.; Yao, H.; Cui, Y. *Chem. Sci.* **2013**, *4*, 3673.
(47) Yuan, L.; Qiu, X.; Chen, L.; Zhu, W. *J. Power Sources* **2009**, *189*, 127.